Landslides (2017) 14:1555–1563
DOI 10.1007/s10346-017-0806-y
Received: 1 July 2016
Accepted: 13 February 2017
Published online: 27 February 2017

A. Dufresne · S. A. Dunning

Process dependence of grain size distributions in rock avalanche deposits

Abstract Rock avalanches are a form of hazardous long-runout landslide and leave fragmented deposits of complex sedimentology that, if studied in detail, can provide insight into their emplacement processes. Complexity arises due to the myriad overlapping factors known to contribute to the final deposit fabric, such as source structures, lithology (i.e. material properties), topographic feedback, substrate interaction and emplacement processes (i.e. internal factors), as well as our reliance on (un)suitable exposures. Herein, we present sedimentological data from two carbonate rock avalanche deposits (Tschirgant in Austria and Flims in Switzerland), where changes in lithology can be eliminated from the causal equation due to their largely mono-mineralic composition. We further eliminated the effects of external influences such as topography or substrate interactions by detailed facies mapping of the deposit interior. Since sedimentary properties locally vary within less than 1-m² outcrop area, emplacement processes are the only causes that remain to explain the different fabrics. Characteristic (fractal) grain size distributions of three distinctive sub-facies in the interior of these, and other, rock avalanche deposits—jigsaw-fractured, fragmented, and shear zone facies—can be linked to specific processes acting during emplacement. We suggest that a heterogeneously distributed and progressively increasing particle breakage in the moving granular mass best explains the ranges of fractal dimensions and associated features for the respective sub-facies, from simple breakage along pre-existing planes, through dynamic fragmentation which locally minimises coordination number, to zones of shear concentration. No exotic emplacement mechanisms (such as air-layer lubrication or fluidised substrates) are required to produce these features; continued, heterogeneous degrees of fragmentation of an initially intact source rock best explains the sedimentary record of rock avalanches.

Keywords Rock avalanche · Facies · Fragmentation · Emplacement processes

Introduction

Rock avalanches are large (>10^6 m^3) highly mobile landslides that result from the sudden failure of rockslopes. The initially relatively intact rock mass is broken during fall and runout, and highly fragmented debris is created and spread over square kilometres within minutes with travel velocities of several 10 m/s. Much effort has focused on elucidating their initiation and emplacement mechanisms (see e.g. Legros 2002) as they often travel much farther than expected. The last decade has seen an increase in sedimentological studies of their deposits (e.g. Crosta et al. 2007; Dunning and Armitage 2011; Weidinger et al. 2014; Dufresne et al. 2016a, 2016b; Zhang et al. 2016). These studies show that there is no average grain size distribution (GSD) that could characterise any given deposit meaningfully as a whole (i.e. for inter-deposit comparison) due to sampling limitations and deposit heterogeneity. Instead, even within small outcrops, a wide span of GSDs and clast arrangements are observed, and differences in the amount of fines from different lithologies seem apparent. What is common and generally scale-independent is that the main interior of deposits with significant runout are composed of fragmented debris (i.e. broken into fragments), and fragmented but relatively undisaggregated clasts—the oft-cited jigsaw puzzle clasts—with the component parts usually angular to very angular (see Weidinger et al. 2014 and references therein). Source stratigraphy is retained despite long runout distances (e.g. Heim 1932; Yarnold and Lombard 1989; Weidinger et al. 2014), and shear bands, faults and block-in-matrix fabrics are common features (e.g. Friedmann 1997; Crosta et al. 2007; Davies and McSaveney 2009; Weidinger et al. 2014; Dufresne et al. 2016b). Three main depositional facies are commonly recognised (see below). However, sedimentological analyses are often based on "bulk" sampling of particular locations regardless of the local, sometimes subtle at outcrop-scale, variations in sedimentology. The aims of those studies were to either characterise a specific deposit GSD for comparison with other deposits or to find trends of e.g. grain size reduction with depth and distance (e.g. Val Pola, Italy, Crosta et al. 2007; Daguangbao, China, Huang et al. 2012; Taranaki, New Zealand, Roverato et al. 2015). During bulk sampling, materials from different facies are collected in one sample, and the detailed information sought in this study are lost as a consequence. Hence, for the purpose of finding information on specific processes responsible for differences in GSD, an alternative approach is proposed herein.

"Facies (Latin 'aspect' or 'appearance' of something) refers to a body of sediment with a distinctive combination of properties that distinguish it from a neighbouring sediment" (Walker 1992 as cited in Evans and Benn 2004; see also Reading 2009). Variations in GSD across the different depositional facies of rock avalanches and rockslides should reflect specific emplacement processes, such as (1) simple fracturing along pre-existing zones of weakness, (2) distributed dynamic fragmentation throughout the moving mass beneath some threshold overburden thickness (McSaveney and Davies 2007), or (3) strain localisation in narrow shear zones, either at the base or in ephemeral layers throughout the body, which could be "inconspicuous" (Davies and McSaveney 2009) in the field. Herein, we apply detailed mapping of rock avalanche sedimentology on the outcrop-scale to identify the different depositional facies before sampling for GSD analyses. It is these details that are needed in order to understand the variations in grain size reduction and hence the processes that are acting within the fragmenting granular mass during rock avalanche emplacement. Therefore, we suggest that sampling for process understanding should be based on prior facies mapping.

We use data from two carbonate rock avalanche deposits: Tschirgant in Austria (Fig. 1b; Prager 2010; Patzelt 2012; Dufresne et al. 2016a) and Flims in Switzerland (Fig. 1a; Pollet and Schneider 2004; Wassmer et al. 2004; Dunning 2004; von Poschinger et al. 2006). Mineral-specific comminution trends (Cintala and Hörz 1992) can be ruled out in these mono-mineralic deposits (peripheral siliciclastic rauhwacken at Tschirgant are herein excluded from analyses). Furthermore, differences in topographic or substrate influence, travel distance, height within the deposit and large-scale source structures can be minimised through facies mapping (see "Methods" below). Therefore, all that remains are the emplacement processes that produced the variable GSDs.

Study sites

The Tschirgant and Flims deposits are amongst the largest rockslide-rock avalanche deposits in the European Alps (Fig. 1). Both originated from carbonate rockslopes, which is the most common source lithology of large, rapid landslides in this mountain belt (Abele 1974). Slope collapse with a drop height of 1400 m of the Tschirgant ridge 3 ka ago (Ostermann et al. 2016) deposited between 180 and 250 mill/m^3 (Abele 1974; Pagliarini 2008; Patzelt 2012) of highly comminuted debris over 9.8 km^2, with a runout of at least 6.8 km (Patzelt 2012). Its deposit contains both linear rocksliding and radial rock avalanche spreading components (Dufresne et al. 2016a). Flims, with a deposit volume of 8–12 km^3 (Heim 1932; von Poschinger et al. 2006), is substantially larger than Tschirgant and dominated by rocksliding emplacement. Its total drop height is 1100 m, covering an area of ~52 km^2 (Heim 1932; Dunning 2004; von Poschinger et al. 2006). Sedimentological investigations of both deposits show that they are multi-facies deposits. We present the facies below.

Methods

Sampling was based on detailed facies mapping, adapting procedures of Glicken (1996): 1-m^2 outcrop areas (mapping windows) were cleaned of slopewash, talus and weathered material, made as planar as possible, then sprayed with water to enhance contrasts and documented by sketches and photographs. Locations of mapping windows were chosen in the carbonate deposit interior to focus on rock avalanche processes only (e.g. avoiding basal zones where mixing with substrates substantially alters debris composition and properties). Each sample was taken from within a specific facies avoiding boundaries with other facies so as to not "contaminate" the sample with material from another facies. A standard phi sieve (16-mm to 63-μm diameter plus receiver pan) tower of woven wire mesh sieves (Retsch) was used and dry-sieving performed using a vibrating table for 10 min. Manual end-point tests of each size fraction were performed: Each sieve was held, still above the next smaller one, at a slightly inclined position and tapped with a metal rod, turned through 90°, tapped, etc. until less than 0.1% of the charge passes through the sieve. Without these endpoint tests, as much as 45% of the material, <63 μm will remain (predominantly) within the 63–250-μm fractions. Sieving was followed by laser diffractometry of material below 250 μm for complete grain size distribution analyses. The laser-sizer results were binned following the phi-scale and integrated with the sieve results. The discrepancy between the two methods lies within only 2–3% (e.g. Beuselinck et al. 1998). Using GSD plots of the equivalent number of grains calculated from the sieve aperture and a density estimate against mean grain size in the Phi interval (after Hooke and Iverson 1995), samples with a heavy-tailed distribution were analysed for self-similar (power-law) behaviour. The statistical methods of Clauset et al. (2009) and Gillespie (2015) were used to assess the significance of the power-law fit, and the size range a fit was valid over. Maximum likelihood estimators were used to determine the values over which behaviour was determined to be self-similar, whilst the goodness of fit was estimated via a Kolmogorov-Smirnov statistic. The result of interest from this procedure here is the fractal dimension, D, the scaling exponent in the power-law relationship.

Rock avalanche facies and grain size distribution

Final rock avalanche deposit fabric and GSD are expected to be heterogeneous since "the state of stress in a deforming granular medium in which grain bridges are continuously forming and breaking is clearly heterogeneous" (Hooke and Iverson 1995, p. 57); yet some common features were found between deposits. Observations of rock avalanche exposures have led to the general consensus on three main deposit facies (Crosta et al. 2007; Dunning and Armitage 2011; Weidinger et al. 2014; Dufresne et al. 2016b): (1) the carapace—an open network of large blocks armouring the deposit surface; (2) the body facies, which makes up the main interior and shows diverse fabrics; and (3) a basal facies in contact, and often mixed or interleaved, with runout path material. The boundary between the basal and the body facies is

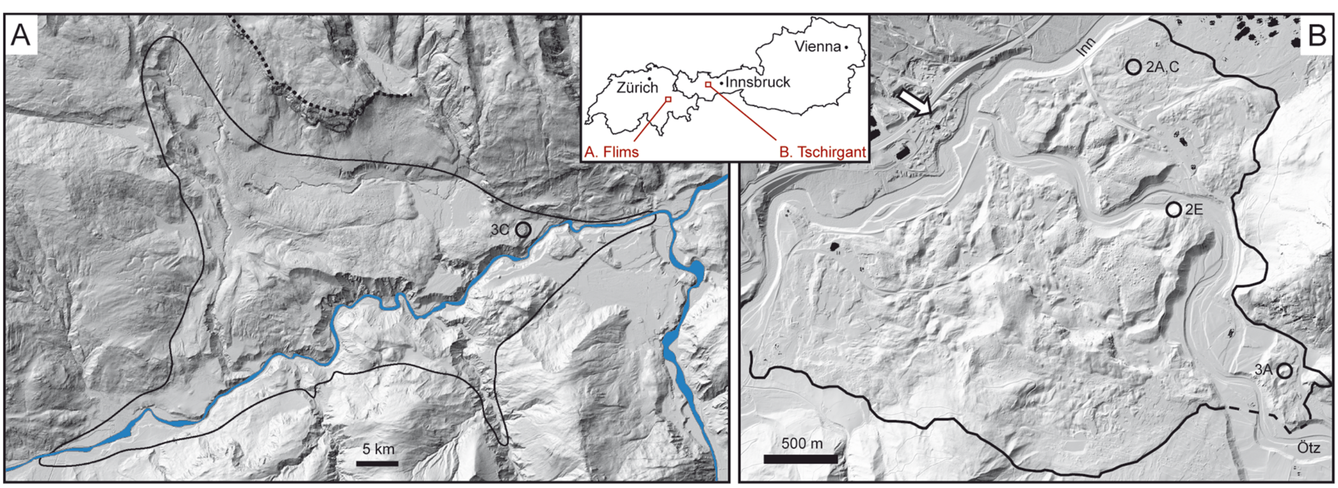

Fig. 1 Location maps of the **a** Flims (LiDAR image from the Federal Office of Topography swisstopo, Switzerland) and **b** Tschirgant deposits (LiDAR image (flights between 2006 and 2010) from the federal government of Tyrol, Austria); *numbers* show where the photos in the respective figures were taken. *Arrow* indicates travel direction

usually sharp, but between the carapace and the body, there is a transitional sub-facies that we have mapped, with clasts still surviving at sizes in excess of the spacing of natural fracture planes or defects—perhaps an explanation for observations of crude inverse grading at outcrop scale exposures (Hungr and Evans 2004).

Features in the body facies are independent of boundary effects such as substrate interactions. Study of this facies allows a focus on the fragmentation processes during runout; particularly because overall clast sizes here are roughly at and below the original joint spacing of the source rock. We designated three sub-facies (Fig. 2a, c, e) for further study, which occur regardless of distance travelled, or height within the deposit. These discrete sub-facies are, at our study sites, not related to variable lithology.

The coarsest sub-facies is the "jigsaw-fractured facies" (Fig. 2a) consisting of angular to very angular clasts up to several cm in size with jigsaw-fit arrangement of individual fragments. Isolated jigsaw-fractured clasts are common in rock and debris avalanche deposits (e.g. Brideau and Procter 2015, and references therein) and are sometimes considered as characteristic and discriminatory for identification purposes. Breaking is usually restricted to failure along pre-existing, inherent, rock-type-specific planes, and their GSD is hence strongly coarse-skewed, with a minor tail of fines that likely originates in the matrix infilling between fracture boundaries (Fig. 2b).

A finer, fragmented facies (Fig. 2c) makes up most of the deposit interior and can be addressed as the "typical" rock avalanche fabric. Comminution transgressing inherent failure planes of the intact rock creates additional surfaces. This facies contains isolated remnant jigsaw-fractured clasts, intact survivor clasts of much larger size than the surrounding majority of fragmented clasts, and clasts with distinctive radial fracturing suggestive of failure originating at point contacts. Grains in the fragmented facies, evidenced by their increasingly more irregular shapes and reduced grain sizes, have experienced more deformation than the jigsaw-fractured clasts. The grain size curve is closer to a bell-shape, as finer materials are relatively more abundant than in the jigsaw-fractured facies, and there are relatively fewer coarser clasts (Fig. 2d).

Finally, extremely fine-grained bands (Fig. 2e), which often stand out by a difference in colour, are identified and interpreted as a shear-zone sub-facies. Shear zones are known in (particularly the basal parts, but also as internal planes) volcanic debris avalanches, rock avalanches and large blockslides, as well as fault zones (e.g. Yarnold and Lombard 1989; van Wyk de Vries et al. 2001; Hewitt 2002; Anders et al. 2000; von Poschinger et al. 2006; Sammis and King 2007; Weidinger et al. 2014). Shear zones display bimodal grain size distributions (Fig. 2f). All these facies may be present within just one square metre outcrop area as our facies mapping revealed (Fig. 3).

In experimental studies (Iverson et al. 1996; Caballero et al. 2014), bimodal distributions develop as a result of increasing shear or confining pressure. Two simultaneous causes might be responsible for this bimodality: (1) Large quantities of fine materials, particularly powders (material <100 μm), are produced through (repeated and/or increased) shearing; (2) the presence of "survivor

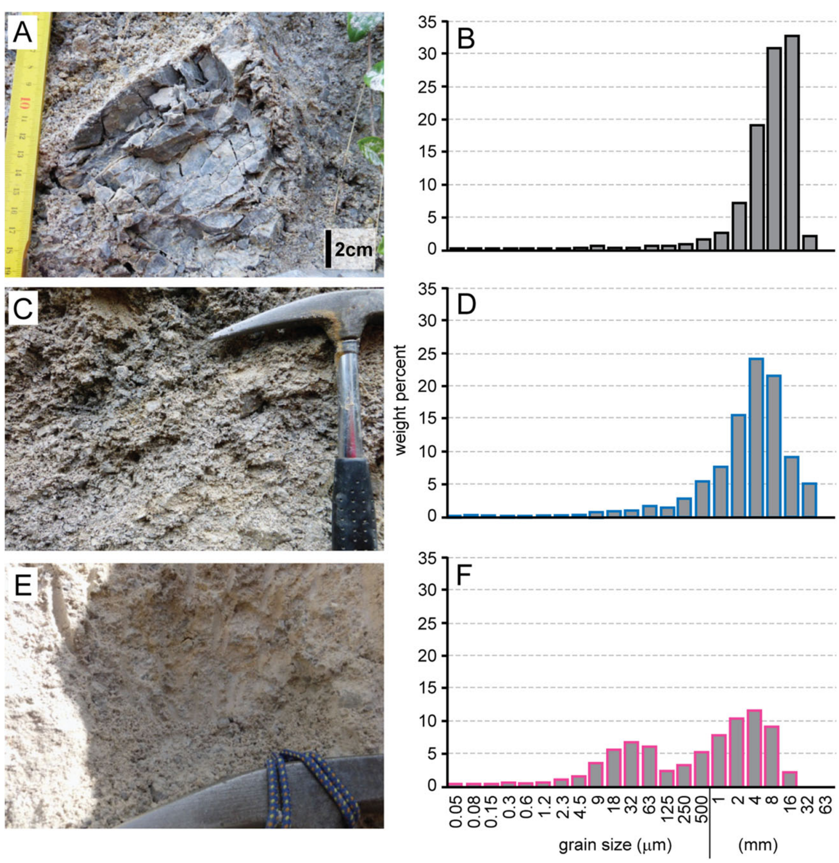

Fig. 2 Rock avalanche facies and their respective, diagnostic grain size distribution histograms (examples from Tschirgant; for sample locations, please refer to Fig. 1). **a**, **b** Jigsaw-fractured clast/facies, **c**, **d** fragmented facies, and **e**, **f** shear bands

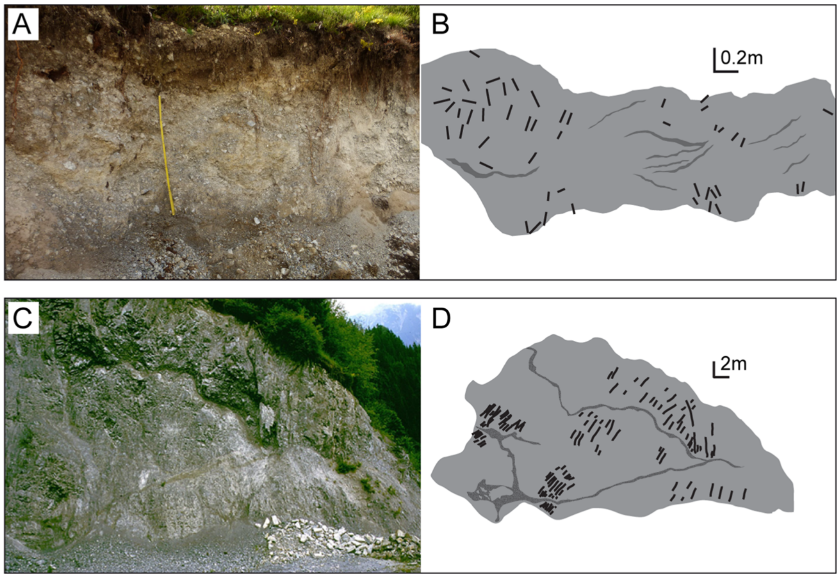

Fig. 3 Facies maps from Tschirgant (**a**, **b**) and Flims (**c**, **d**) rock avalanche deposits showing the close spatial proximity of the different facies. The dominant facies is the fragmented facies (*lighter grey*); shear zones (*dark grey*) appear throughout the deposits. The orientations of *black lines* of the jigsaw-fractured facies indicate a somewhat more ordered fabric within the Flims deposit due to strong source structure influence on facies development (although Tschirgant shows evidence of fracture development predominantly following emplacement direction)

grains" (Storti et al. 2007) that remain unbroken due to armouring by smaller adjacent particles breaking preferentially. This cushioning effect (Sammis et al. 1987; Tsoungui et al. 1999) underlies the fact that the largest grain can remain uncrushed, since to break it requires grains of equal or larger size than the grain being crushed, if all grains have the same material strength (Davies and McSaveney 2009). The occurrence of larger clasts in an overall fine material is an inherited feature providing evidence of continued, size/packing selective fragmentation. GSD curves derived from experimental crushing of granular materials also show survivor clasts; hence, the largest sizes are never completely lost despite continued crushing or shearing (Fig. 4c, d).

Comparing the GSD curves of Tschirgant and Flims (Fig. 4a, b) with data from granular shear experiments (Fig. 4c, d) supports the idea of increased grain crushing across our three observed subfacies. The jigsaw-fractured facies is closest to a virtual "initial distribution" (i.e. closer to joint spacing at the source), the fragmented facies results from higher shear strain and/or repeated crushing, and finally, shear bands experience the highest degree of fragmentation. After prolonged shearing, i.e. larger shear strain, or

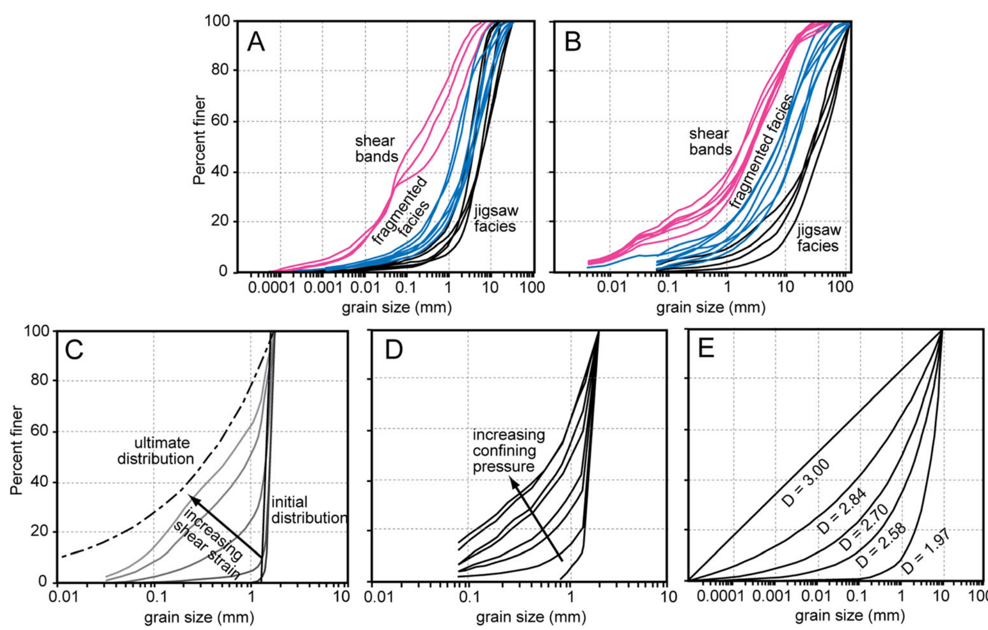

Fig. 4 Grain size distribution data from field and experiment. **a** Tschirgant. **b** Flims rock avalanches. **c**, **d** Shifts in GSD curves towards an "ultimate distribution" with increasing shear strain in experiments by Einav (2007) and Lade et al. (1996), respectively. **e** Synthetic GSD computed with different *D*-values (Crosta et al. 2007)

at increasing confining pressure, an "ultimate grain size distribution" (Einav 2007) or "practical maximum density curve" (Lade et al. 1996) might be approximated (Fig. 4c, d). What this ultimate distribution may look like for a rock avalanche is unknown, if it exists at all. At Tschirgant and Flims, there is still evidence of "incomplete" fragmentation at all sample localities, with fractal dimensions remaining well below the theoretical computation by Crosta et al. (2007) of an ultimate distribution with a fractal dimension (*D*) of 3.0 (Fig. 4e).

Fractal dimensions

Comminuted rock avalanche deposits have been found to be fractal/self-similar in (destructive) samples—a sampling style we also used. However, the nature of sampling does not consider in situ clast arrangement, i.e. a value of *D* that can theoretically be related to that maximising the spacing between fragments of a similar size does not necessarily evidence that this was the 3D clast configuration. The *D*-value from destructive sampling is still a useful proxy for a bulk estimate of the degree of fragmentation and relationships between clast sizes in the sampled volume. The methods of Clauset et al. (2009) were applied to all samples, as each initially appears to approximate a fractal distribution. A range of methods have been used in the literature to determine *D* and how well a power-law describes data. Often, an R^2 value for a power-law fit, or a linear fit to log-transformed data, with little evaluation of the goodness of fit or statistical analyses of what parts of the GSD can be defined as fractal (i.e. the upper and lower fractal bounds) is reported. For our data, no samples, or limited size ranges within samples using the methods of Clauset et al. (2009), could be fitted by a statistically significant power-law distribution (Fig. 5). The cumulative density estimates show significant deviation from a power-law in the 0.2–0.001-mm range, and there is an excess of clasts as compared to predicted distributions, often with a peak at around 0.02 mm. Outside of this range, data appear best approximated by a number of discrete power-law regions, coarse clasts by a lower *D*-value fit, the fine clast size by a higher *D*-value fit, but as a caveat, there are not enough data in these ranges to statistically validate this fit. In addition, the finer clast sizes are measured based on laser diffraction which assumes a spherical particle, whilst the large clasts from sieve analyses are considered a measure of the *b*-axis and can be heavily shape-dependent.

In all cases, our data do fit a power-law distribution when using a linear fit to log-transformed data (Fig. 5a) with R^2 values in excess of 0.9 and with *D*-values always higher than those estimated using maximum-likelihood analyses—where the fit was not deemed significant. Despite this being perhaps less rigorous, we report them here as comparative values of increasing comminution intensity (Storti et al. 2007) or damage (Nakata et al. 2001), and to compare our values with those previously reported in the literature for rock avalanche deposits, experiments, and theoretical computations. This shift from rejection of a power-law fit to these data, to acceptance for all samples with a high goodness-of-fit value, questions the validity of the fractal nature, specific *D*-values or fractal ranges for many rock avalanche GSDs published, and some of the interpretations linked to this where *D*-values have theoretical links, e.g. to fragmentation probabilities.

Increasing particle breakage is reflected in the *D*-values of our samples, which increase from the jigsaw-facies, to the fragmented facies (which clusters just below 2.58 and within "typical" values for rock avalanche interiors (e.g. Crosta et al. 2007)), to shear zones (Fig. 6). The differences in data scatter and range of fractal dimensions of the two deposits might have a twofold reason: (1) The facies-mapping approach was refined between sampling Flims (Dunning 2004) and Tschirgant (Dufresne et al. 2016b), and might hence emphasise the importance of appropriate and comparable sampling strategies; (2) Flims is dominated by rocksliding and underwent significant collision with the opposing valley walls, an interference that is suspected to reduce clast comminution by halting motion and hence fragmentation prematurely (Hewitt 2001). Alternatively, collision may generate intense elastic impact waves that increase comminution. Nevertheless, the general *D*-value trend across the different facies is the same for both deposits, and *D*-value ranges overlap sufficiently.

A *D*-value of 2.58 theoretically approximates an in situ packing arrangement that maximises coordination number and so minimises the probabilities of fragmentation, since clasts of similar size are effectively cushioned from each other by a range of particle sizes surrounding them (Sammis et al. 1987)—hence the longevity of survivor clasts. The *D*-values in our deposits approximate those of Storti et al. (2007) for brecciated fault rocks (dashed vertical grey lines in Fig. 6), and our shear band values overlap with those of shear zones in fault rocks (solid vertical grey lines in Fig. 6); there is a close similarity of processes between tectonic fault zones, rock avalanches and experimental shearing/crushing that crosses several orders of magnitude.

Process identification

The facies-GSD data presented herein offer a useful tool for the identification of emplacement processes in rock avalanches. In mono-mineralic deposits, the model is very simple. It documents the progression from simple breakage along pre-existing planes of weakness (jigsaw-fractured facies) to fragmentation that transgresses original failure planes and creates new surfaces (fragmented facies), to zones of shear concentration (shear bands). Any sampled GSD histogram and curve can be attributed to these breakage processes (Figs. 2 and 7a, b). They may occur at any location in the runout (Fig. 7c), in addition to progressive comminution trends along the runout path as observed for some volcanic debris avalanches (Roverato et al. 2015; Perinotto et al. 2015) and searched for in rock avalanches where GSD curves "become progressively more widely graded" (Crosta et al. 2007). For example, jigsaw-fractured clasts may form early during emplacement but be subsequently broken down into smaller clasts, progressively transforming into the fragmented facies. Other jigsaw-fractured clasts are formed later and are preserved in the final deposits. Shear bands may form within debris of the fragmented facies, progressively and locally reducing grain sizes here. Hence, all processes act throughout the entire granular mass and throughout the entire emplacement duration. Progressive facies development was also documented by Dufresne et al. (2016b) who identified slight "maturation" in histograms within the same facies from proximal to distal sample locations. This suggests that progressive grain size reduction trends reported in the literature may not only be a function of bulk sampling, including varying relative amounts of different facies types, but that fragmentation within each facies progresses with distance travelled, thereby (a) increasing the relative proportion of the finer-grained facies with distance and (b) pushing each individual facies towards overall smaller grain sizes, which agrees with the

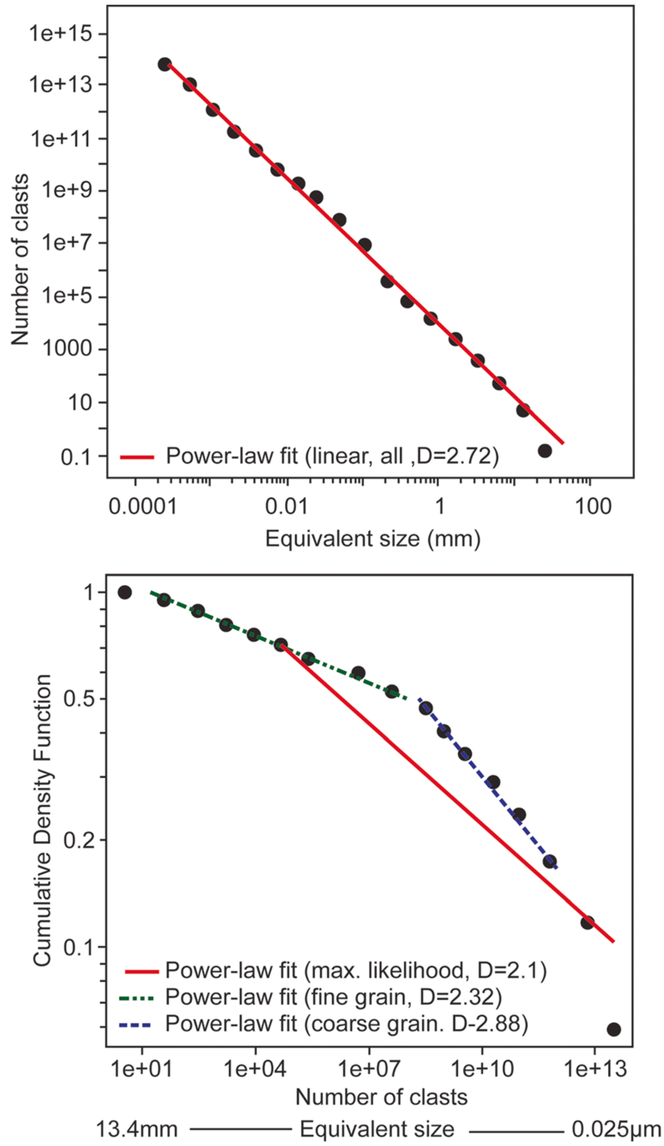

Fig. 5 **a** Commonly used linear fit to log-transformed GSD data to determine the fractal dimension (D), with good agreement of one D-value (2.72) over the entire size range analysed with $R^2 > 0.99$. **b** Power-law fitting using maximum-likelihood estimators and a Kolmogorov-Smirnov test to the same data as **a**. No statically valid D-value can be derived for the full GSD (the rejected best fit power-law returns $D = 2.1$), and two discrete size-dependent power-law fit regions emerge

experimental findings discussed above. The facies-approach furthermore shows potential to serve as a tool to identify combinations of processes, influencing factors, and predominance of one process over another (e.g. related to the runout path; see Dufresne et al. 2016b), and through the study of poly-mineralic deposits, how complex source stratigraphy partitions strain and fragmentation during emplacement.

Since the three sub-facies identified herein can be found in all locations confirms that fragmentation is on-going throughout runout (previously alluded to by Davies et al. 1999; Hewitt 2002); this has emplacement implications. The moving mass is not passively travelling over a basal shear plane, but rather, shear is distributed throughout the mass for the duration of motion, often localising in some narrow zones—our shear facies. Therefore, pure basal sliding (on e.g. melt, nanoparticles, air, or fluidised substrate) alone does not explain long runout. Any emplacement hypothesis that aims at not only predicting runout distances based on stress/friction parameter variation, but which also attempts to explain the underlying mechanical processes, must include heterogeneous stress distributions and continuing fragmentation throughout most of the flow length, thickness and emplacement duration. A number of hypotheses to explain long runout have been proposed and include (1) dynamic fragmentation (Davies 1982; Davies and McSaveney 2009), (2) acoustic fluidization (Melosh 1979), (3) pressure variations (Johnson et al. 2016), (4) multi-slide plug flow (Roverato et al. 2015), (5) plug or viscous flow (Voight et al. 1983; Kelfoun and Druitt 2005), (6) a lubricating basal layer (Campbell 1989) or (7) undrained loading of the underlying saturated sediments (Hutchinson and Bhandari 1971). These hypotheses all agree with preservation of stratigraphy in the deposits since none evokes turbulence within the granular flow. Formation of a carapace above a deforming granular body is also agreeable

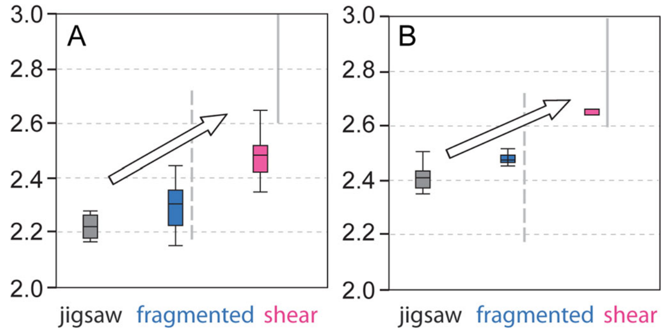

Fig. 6 Number-size plots showing *D*-value development with facies for **a** Flims and **b** Tschirgant. *Vertical grey lines* indicate *D*-value ranges of brecciated (*dashed*) and shear zone (*solid*) fault rocks (Storti et al. 2007)

with all of them. Some of the hypotheses, however, require reduction of frictional resistance in a basal layer (5, 6, 7); hence, all observed basal deformation, including substrate erosion, entrainment and mixing, is accounted for. But, also those hypotheses without focus on basal layer deformation do not oppose explanation of these phenomena, simply based on the boundary dynamics of granular flows over deformable substrates.

Explanations of the internal granular facies as described in this paper might limit some of the hypotheses. Jigsaw-fractured clasts require differential stresses and pressures that are low enough and not in disagreement with most models of a dynamically deforming granular body. Processes to produce the fragmented facies, however, require higher stresses and pressures best explained by the dynamic fragmentation model. Acoustic fluidization alone does neither require nor cause dynamic particle breakage, nor would basal layer processes necessarily induce stresses within the overlying granular mass that are high enough for particles to break along newly formed surfaces. The most important observation in our facies model is that shear is not restricted to a basal layer but distributed throughout the entire rock avalanche body (beneath sufficient overburden, thereby exempting the carapace, naturally). This is supported by the dynamic fragmentation hypothesis (Davies 1982; Davies and McSaveney 2009), the pressure variations modelled by Johnson et al. (2016), acoustic fluidisation (Melosh 1979), and is observed in the more empirical multi-slide plug flow model (Roverato et al. 2015; an extension of the plug-flow model).

We can conclusively exclude exotic processes (such as air-layer lubrication) since they do not explain the observed sedimentological features. Likewise, sliding on a thin film of melt is not a viable candidate to explain long runout since only few RS/RAs contain frictionites (e.g. Erismann 1979) and the films are too thin and viscous to support rapid motion of a large overburden. Furthermore, observations at the Köfels rockslide in Austria suggest that frictionites may simply be an expression of shear concentration since they are found in extension of fine-grained shear zones within the deposit.

The surface of thick rock avalanches, on the other hand, tells us nothing of the interior arrangement of facies. It rather indicates the degree and geometry of spreading of the debris (e.g. Dufresne et al. 2016a).

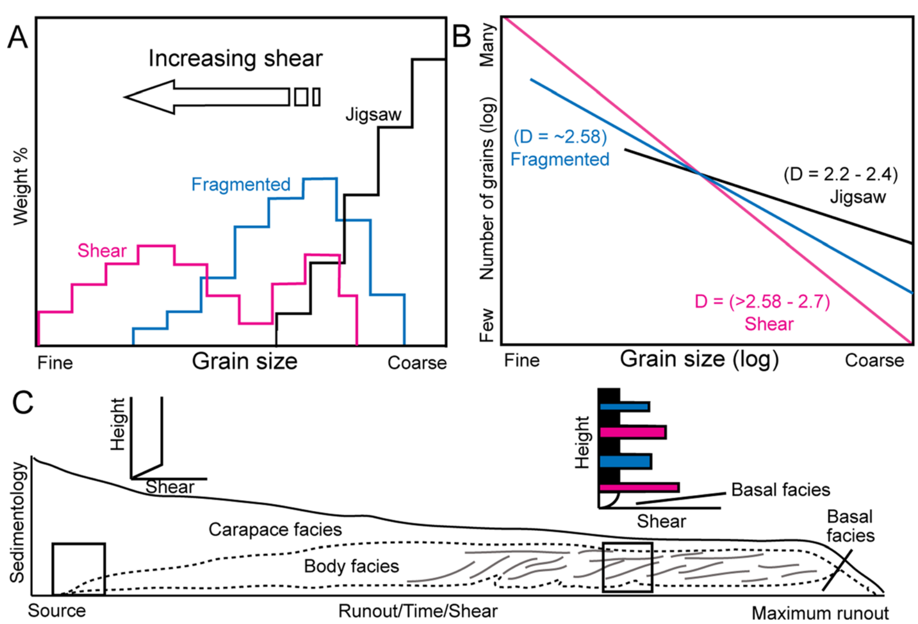

Fig. 7 Conceptual sketches. **a**, **b** GSD and *D*-value shifts in rock avalanches. **c** Conceptual sketch of facies distribution

Conclusions

This present study systematically addressed uncertainties regarding sampling and GSD analyses of rock avalanche deposits. Our results particularly emphasise a need for improved sampling strategies if information about fragmentation processes and spatial distribution of grain size changes within the RA is sought. Therefore, sampling strategies should be based on prior facies mapping if we truly want to understand the processes underlying rock avalanche emplacement. Each facies produces a unique grain size distribution, and their histograms can serve as a tool for facies/process identification and for sensible comparison between deposits and lithologies. Our results support a small number of emplacement theories and rule out any exotic explanation for the long runout of large rock avalanches; continued, heterogeneous degrees of fragmentation of an initially relatively intact source rock best explains the sedimentary record of rock avalanches. They furthermore serve to refine numerical models (e.g. heterogeneous stress distribution as input parameter) and, as Hutchinson (2006) generally stated about the value of sedimentological studies of rock avalanches, to "counteract any tendency for modelling to run ahead of field observations".

Acknowledgements

This research was partially funded by the German Research Foundation grant DU1294/2-1 to AD. We gratefully acknowledge thorough review by the editor Mauri McSaveney and by two anonymous reviewers. AD is indebted to Christoph Prager for abseiling during sample collection at Tschirgant.

References

Abele G (1974) Bergstürze in den Alpen, ihre Verbreitung, Morphologie und Folgeerscheinungen. Wissenschaftliche Alpensvereinshefte 25:230

Anders MH, Aharonov E, Walsh JJ (2000) Stratified granular media beneath large slide blocks: implications for mode of emplacement. Geology 28(11):971–974

Beuselinck L, Govers G, Poesen J, Degraer G, Froyen L (1998) Grain-size distribution by laser diffractometry: comparison with the sieve-pipette method. Catena 32:193–208

Brideau M-A, Procter JN (2015) Discontinuity orientation in jigsaw clasts from volcanic debris avalanche deposits and implications for emplacement mechanism. GeoQuébec 2015:20–23 Abstract 614

Caballero L, Sarocchi D, Soto E, Borselli L (2014) Rheological changes induced by clast fragmentation in debris flows. J Geophys Res: Earth Surf 119(9):1800–1817

Campbell CS (1989) Self-lubrication for long runout landslides. J Geol 97(6):653–665

Cintala MJ, Hörz F (1992) An experimental evaluation of mineral-specific comminution. Meteoritics 27:395–403

Clauset A, Shalizi CR, Newman MEJ (2009) Power-law distributions in empirical data. SIAM Rev 51(4):661–703

Crosta GB, Frattini P, Fuis N (2007) Fragmentation in the Val Pola rock avalanche, Italian Alps. J Geophys Res 112:23

Davies TR (1982) Spreading of rock avalanche debris by mechanical fluidization. Rock Mech 15(1):9–24

Davies TR, McSaveney MJ (2009) The role of rock fragmentation in the motion of large landslides. Eng Geol 109:67–79

Davies TR, McSaveney MJ, Hodgson KA (1999) A fragmentation-spreading model for long-runout rock avalanches. Can Geotech J 36:1096–1110

Dufresne A, Prager C, Bösmeier AS (2016a) Insights into rock avalanche emplacement processes by detailed morpho-lithological studies of the Tschirgant deposit (Tyrol Autria). Earth Surf Process Landf 41(5):587–602

Dufresne A, Bösmeier AS, Prager C (2016b) Rock avalanche sedimentology – case study and review. Earth-Sci Rev 163:234–259

Dunning S (2004) Rock avalanches in high mountains [PhD thesis]. University of Luton, UK:309

Dunning SA, Armitage PJ (2011) The grain-size distribution of rock-avalanche deposits: implications for natural dam stability. In: Evans SG, Hermanns RL, Strom A, Scarascia-Mugnozza G (eds), Natural and Artifical Rockslide Dams, Lecture Notes in Earth Sciences 133:479–498

Einav I (2007) Breakage mechanics – part II: modelling granular materials. J Mech Phys Solids 55:1298–1320

Erismann TH (1979) Mechanisms of large landslides. Rock Mech 12(1):15–46

Evans DJA, Benn DI (2004) Facies description and the logging of sedimentary exposures. In: Evans DJA, Benn DI (eds) A practical guide to the study of glacial sediments. Routledge, Taylor & Francis Group, New York, pp 11–51

Friedmann SJ (1997) Rock-avalanche elements of the Shadow Valley basin, eastern Mojave Desert, California: processes and problems. J Sediment Res 67(5):792–804

Gillespie CS (2015) Fitting heavy tailed distributions: the poweRlaw package. J Stat Softw 64(2). doi:10.18637/jss.v064.i02

Glicken H (1996) Rockslide-debris avalanche of May 18, 1980, Mount St. Helens, Washington. USGS Open-file Report 96–677:90 pp

Heim A (1932) Bergsturz und Menschenleben (Landslides and human lives). Vierteljahrsschrift der Naturforschenden Gesellschaft in Zürich 77. Beer & Co, Zürich 218 pp

Hewitt K (2001) Catastrophic rockslides and the geomorphology of the Hunza and Gilgit river valleys, Karakoram Himalaya. Erdkunde 55:72–93

Hewitt K (2002) Styles of rock avalanche depositional complexes conditioned by very rugged terrain, Karakoram Himalaya, Pakistan. Rev Eng Geol 15:345–377

Hooke RLEB, Iverson NR (1995) Grain-size distribution in deforming subglacial tills: role of grain fracture. Geology 23(1):57–60

Huang R, Pei X, Fan X, Zhang W, Li S, Li B (2012) The characteristics and failure mechanism of the largest landslide triggered by the Wenchuan earthquake, may 12, 2008, China. Landslides 9:131–142

Hungr O, Evans SG (2004) Entrainment of debris in rock avalanches: an analysis of a long runout-out mechanism. Geol Soc Am Bull 116(9–10):1240–1252

Hutchinson JN (2006) Massive rocks slope failure: perspectives and retrospectives on state-of-the-art. IN: Evans SG, Scarascia-Mugnozza G, Strom AL, Hermanns RL (eds) Landslides from Massive Rock Slope Failure. Nato Science Series IV, Earth and Environmental Sciences 49:619–662

Hutchinson JN, Bhandari RK (1971) Undrained loading, a fundamental mechanism of mudflows and other mass movements. Géotechnique 21:353–358

Iverson NR, Hoover TS, Hooke RL (1996) A laboratory study of sediment deformation: stress heterogeneity and grain-size evolution. Ann Glaciol 22:167–175

Johnson BC, Campbell CS, Melosh HJ (2016) The reduction of friction in long runout landslides as an emergent phenomenon. J Geophys Res, Earth Surf. doi:10.1002/2015JF003751

Kelfoun K, Druitt TH (2005) Numerical modeling of the emplacement of Socompa rock avalanche, Chile. J Geophys Res B: Solid Earth 110(12):1–13

Lade PV, Yamamuro JA, Bopp PA (1996) Significance of particle crushing in granular materials. J Geotech Eng 122(4):309–316

Legros F (2002) The mobility of long-runout landslides. Eng Geol 63:310–331

McSaveney MJ, Davies TR (2007) Rockslides and their motion. In: Sassa K, Fukuoka H, Wang F, Wang G (eds) Progress in landslide science. Springer-Verlag, Berlin, pp 113–134

Melosh HJ (1979) Acoustic fluidization – a new geologic process. J Geophys Res 84(B13):7513–7520

Nakata Y, Hyodo M, Hyde AFL, Kato Y, Murata H (2001) Microscopic particle crushing of sand subjected to high pressure one-dimensional compression. Soils Found 41(1):69–82

Ostermann M, Ivy-Ochs S, Sanders D, Prager C (2016) Multi-method (^{14}C, ^{36}Cl, ^{234}U/^{230}Th) age bracketing of the Tschirgant rock avalanche (eastern alps): implications for absolute dating of catastrophic mass-wasting. Earth Surf Process Landf. doi:10.1002/esp.4077

Pagliarini L (2008) Strukturelle Neubearbeitung des Tschirgant und Analyse der lithologisch-strukturell induzierten Massenbewegung (Tschirgant Bergsturz, Nördliche Kalkalpen, Tirol). Diplom thesis. Leopold-Franzens-Universität Innsbruck, Austria:95 pp

Patzelt G (2012) The rock avalanches of Tschirgant and Haiming (upper Inn Valley, Tyrol, Austria), comment on the map supply. Jahrb Geol Bundesanst 152(1–4):13–24

Perinotto H, Schneider J-L, Bachèlery P, Le Bourdonnec F-X, Famin V, Michon L (2015) The extreme mobility of debris avalanches: a new model of transport mechanism. J Geophys Res: Solid Earth. doi:10.1002/2015JB011994

Pollet N, Schneider J-LM (2004) Dynamic disintegration processes accompanying transport of the Holocene Flims Sturzstrom (Swiss Alps). Earth Planet Sci Lett 221:433–448

Prager C (2010) Geologie, Alter und Struktur des Fernpass Bergsturzes und tiefgründiger Massenbewegungen in seiner Umgebung. PhD thesis, Universität Innsbruck, Tirol, Österreich, p 307

Reading HG (ed) (2009) Sedimentary environments: processes, facies, and stratigraphy. Oxford, Blackwell, 689 pp

Roverato M, Cronin S, Procter J, Capra L (2015) Textural features as indicators of debris avalanche transport and emplacement, Taranaki volcano. GSA Bull 127(1–2):3–18

Sammis C, King G (2007) Mechanical origin of power law scaling in fault zone rock. Geophys Res Lett 34:L04312. doi:10.1029/2006GL028548
Sammis CG, King G, Biegel RL (1987) The kinematics of gouge deformation. Pure Appl Geophys 125:777–812
Storti F, Balsamo F, Salvini F (2007) Particle shape evolution in natural carbonate granular wear material. Terra Nov. 19:344–352
Tsoungui O, Vallet D, Charmet J-C (1999) Numerical model of crushing of grains inside two-dimensional granular materials. Powder Technol 105:190–198
van Wyk de Vries B, Self S, Francis PW, Keszthelyi L (2001) A gravitational spreading origin for the Socompa debris avalanche. J Volcanol Geotherm Res 105:225–247
Voight B, Janda RJ, Glicken H, Douglass PM (1983) Nature and mechanics of the Mount St. Helens rockslide-debris avalanche of 18 may 1980. Géotechnique 33(3):243–273
von Poschinger A, Wassmer P, Maisch M (2006) The Flims rockslides: history of interpretation and new insights. In: Evans SG, Scarascia MG, Strom A, Hermanns RL (eds), Landslides from massive rock slope failure, NATO Science Series, IV, Earth and Environmental Sciences 49:329–256
Walker RG (1992) Facies, facies models and modern stratigraphic concepts. In: Walker RG, James NP (eds) Facies models: response to sea-level change. Geological Association of Canada, Toronto, pp 1–14
Wassmer P, Schneider JL, Pollet N, Schmitter-Voirin C (2004) Effects of the internal structure of a rock-avalanche dam on the drainage mechanism of its impoundment, Flims Sturzstrom and Ilanz paleo-lake, Swiss Alps. Geomorphology 61:3–17
Weidinger JT, Korup O, Munack H, Altenberger U, Dunning S, Tipelt G, Lottermoser W (2014) Giant rockslides from the inside. Earth Planet Sci Lett 389:62–73
Yarnold JC, Lombard JP (1989) A facies model for large rock avalanche deposits formed in dry climates. In: Colburn IP, Abbott PL, Minch J (eds) Field Trip Guidebook - Pacific Section, Society of Economic Paleontologists and Mineralogists 62:9–31
Zhang M, Yin Y, McSaveney M (2016) Dynamics of the 2008 earthquake-triggered Wenjiagou Creek rock avalanche, Qingping, Sichuan, China. Eng Geol 200:75–87

A. Dufresne (✉)
Engineering Geology and Hydrogeology,
RWTH Aachen University,
Aachen, Germany
e-mail: dufresne@lih.rwth-aachen.de

S. A. Dunning
School of Geography, Politics and Sociology,
Newcastle University,
Newcastle, UK
e-mail: stuart.dunning@newcastle.ac.uk